Journal of Electrical Engineering, Vol. 77, No. 4, 2026, pp. 392-403
https://reference-global.com/journal/JEE

An efficient codebook design approach based on salp swarm algorithm for the downlink SCMA system

Şakir Şimşir

The codebooks are the key components of the sparse code multiple access (SCMA) system. In order to distinguish the multiple users from one another, a distinct codebook is assigned to each user. Apart from this, the codebook design has a direct effect on the SCMA performance. In other words, a properly designed codebook set leads to a performance boost in the SCMA system. For this reason, it is crucial to find the most appropriate codebook set to maximize the system performance. With that purpose in mind, a salp swarm algorithm (SSA)-based codebook design scheme has been proposed for the downlink SCMA system in this paper. In the proposed scheme, the codebooks are directly optimized by a recently developed robust algorithm called SSA to acquire the ideal codebook set for the related system. Most of the codebook design procedures available in the literature consider some key performance indicators like minimum product distance (MPD) and minimum Euclidean distance (MED) of the superimposed codewords while designing the codebook set. However, the system performance represented by the average bit error rate (BER) of the multiple users cannot only be determined by the distance properties of the superimposed codewords but also affected by the symbol detector by which the information bits are recovered using the designed codebook set at the receiver side. For this reason, in order to take the whole system into account without concentrating solely on the distance characteristics of the codewords, the average BER value of the SCMA scheme is employed as a fitness function of SSA to be minimized while optimizing the codebook set. In the simulation study, the BER achievement of the proposed SSA-based codebook design strategy is compared to those of varied methods existing in the literature. According to the simulation results, the codebook set produced by the suggested strategy makes the downlink SCMA system to reach better BER levels compared to the other methods considered in this paper.

Keywords: sparse code multiple access (SCMA), salp swarm algorithm (SSA), codebook design, non-orthogonal multiple access (NOMA), sixth generation (6G)

1 Introduction

It is not hard to predict that we are approaching the sixth generation (6G) era even though the fifth generation (5G) mobile technology has not yet been fully deployed throughout the world [1]. According to the vision determined by the International Telecommunication Union (ITU), 5G systems are expected to meet three typical scenarios like massive machine type communication (mMTC) allowing one million connections per square kilometer (km^2), enhanced mobile broadband (eMBB) systems ensuring data speeds in the order of gigabits per second and ultra reliable low latency communication (URLLC) systems providing milli-second latency in the air interface. Furthermore, the new applications that have emerged in recent years such as autonomous driving, virtual reality (VR), 3D integrated communications and augmented reality (AR) seem likely to accelerate the transition from 5G to 6G. In the aforementioned scenarios, communication access at extremely high speeds and far more data rates which exceed those offered by 5G technology is going to be needed in the upcoming period [2]. Satisfying such endless high standard communication scenarios will become challenging unless more sophisticated transmission technologies are developed. The inventions of multiple access schemes like time division multiple access (TDMA), code division multiple access (CDMA), frequency division multiple access (FDMA) and orthogonal frequency division multiple access (OFDMA) have been the most significant milestones in the progress of wireless technology throughout different generations [3, 4]. The common fundamental principle behind these multiple access strategies, each of which has been employed in a different generation of mobile technology, is orthogonality. According to the principle of orthogonality, resource sharing is carried out orthogonally among the multiple users in frequency, code or time domain. We can both minimize the multiple access interference and employ low-complexity receivers by performing an orthogonal assignment of resource blocks between the users.

From the other point of view, the existing orthogonal resource blocks cause a restriction in the number of manageable users. For this reason, the orthogonal-based multiple access technologies will not be sufficient to satisfy the growing connectivity demands that are expec-

Nevşehir Hacı Bektaş Veli University, Department of Electrical and Electronics Engineering, Nevşehir, Türkiye
E-mail: sakirsimsir@nevsehir.edu.tr

https://doi.org/10.2478/jee-2026-0038, Print (till 2015) ISSN 1335-3632, On-line ISSN 1339-309X

ted to intensify even more in the future generations. Taking this into account, the researchers developed a non-orthogonal multiple access (NOMA) [5-7] scheme to pave the way for widespread access. Thanks to this non-orthogonal technology, the resource blocks can be further exploited. For instance, in the NOMA system, it is possible for multiple users to share the identical narrow frequency range within the same time frame. This enables supporting additional number of users while leading to an enhancement in the complexity of the receiver. There are two primary NOMA categories regarding the types of allocated resources. These are code domain and power domain NOMAs called CD-NOMA and PD-NOMA, respectively. While PD-NOMA makes use of power as a new dimension, CD-NOMA applies a similar approach with the traditional CDMA. The usage of spreading codes that are limited to non-orthogonal sparse sequences with low cross correlation is the key difference of CD-NOMA compared to CDMA [8-10].

CD-NOMA category includes an exclusive member of multiple access schemes called sparse code multiple access (SCMA) [11], which has been drawing considerable attention in recent years due to its great potential to be employed in future generations of mobile communication systems. In the SCMA system, the spreading operation is combined with the modulation process. A set of codebooks pre-defined in the SCMA scheme consists of multi-dimensional complex codewords. These codewords are selected from the codebook set with respect to the information bits of the related user. It is possible for the SCMA system to provide a notable shaping gain due to the usage of high-dimensional sparse codebooks. Furthermore, inherent sparsity of the SCMA scheme allows for easy implementation of advanced message passing algorithm (MPA) at the receiver side for the multiuser detection process [12].

On the other hand, the bit error rate (BER) achievement of the SCMA system is directly influenced by the design of a codebook set. In other words, it is possible to maximize the system performance by designing the codebook structure, appropriately. The study carried out in this paper addresses this matter referred to as codebook design in literature. Within this scope, the codebook design issue is transformed into an optimization problem by making the codebooks of multiple users suitable for being optimized in a direct manner. With view to fulfilling the related optimization task, an efficient recently developed metaheuristic approach called salp swarm algorithm (SSA) [13] is proposed. After fulfilling the codebook optimization process carried out for the Rayleigh fading channel in the downlink SCMA system, the BER performance of theSSA-based optimized codebook set is compared withthose of varied codebook sets existing in the literature. It is evidently demonstrated by the comprehensive experimental analysis that the proposed SSA-based strategy is a promising codebook design approach to be utilized in the downlink SCMA system due to its superior BER performance compared to the other considered tech-niques.

The literature includes diversified studies focusing on the design of an appropriate set of codebooks for the SCMA scheme. In [14], a strategy of codebook design that relies on the star quadrature amplitude modulation (StarQAM) constellations is developed. In [15], the design of the codebook set is carried out by utilizing the genetic algorithm (GA). Since the GA is directly applied to the codebooks of multiple users, the mother constellation is not required for the optimization process. While optimizing the codebook set, minimum Euclidean distance (MED) is employed as the objective function to be maximized by the GA. The studies carried out in [16] and [17] are based on the maximization of MED, which is a key performance indicator providing significant information about the BER achievement of the related codebook set particularly in the additive white Gaussian noise (AWGN) channel. In [18], in order to further increase the MED between the superimposed codewords existing in the set of codebooks, the authors reformulate the MED problem into a biconvex form by implementing an iterative algorithm based on alternating maximization. In [19], the authors consider the energy diversity of the constellation points along with the MED when acquiring the optimum codebook collection for the SCMA system. In [20], a sub-optimal technique is proposed to construct an improved SCMA codebook set for varied uplink Rician fading scenarios. In [21], the authors design a novel class of codebooks, which demonstrates a power imbalance among multiple users, by considering not only the MED but also the minimum product distance (MPD) of the codewords during the design process. In [22] and [23], the codebook design is performed in two stages. In the first stage, the optimum codebook is designed for a single user. In the following stage, the relevant codebook designed in the previous stage is subjected to some user-specific operations to achieve the codebooks of the remaining users. In [24], a combined multitask learning-based framework, in which the authors utilize deep learning to jointly design decoder and encoder blocks of the SCMA scheme, is proposed. In [25], a deep neural network-based new approach is put forward by the authors with a view to design a useful codebook set for the SCMA system.

It is possible to summarize the key contributions of this study in the following way:

1. In the literature, it is the first time for the salp swarm algorithm to be integrated into the SCMA scheme with the aim of resolving the codebook design issue.
2. In this paper, instead of focusing our attention solely on the transmitter side of the SCMA scheme by taking only the distance properties of the codewords into account, we consider the whole system with each component having an impact on the BER performance while designing the codebook set. To this end, we determine the average BER of the SCMA system as the objective function of SSA for being minimized rather than maximizing the MPD or MED of the codewords as is done in most codebook design works. By doing so, not only the transmitter, but also the receiver side of the SCMA scheme where the logarithmic-message passing algorithm (log-MPA) detector has a significant effect on the system performance is taken into account while optimizing the codebook set via the SSA.
3. The SSA-based codebook set designed for the downlink SCMA system evidently gets ahead of various prominent codebook sets such as AESCMA [25], LowError [18], Hu [26], Huawei and ConsRot [27] with regard to BER performance in the related system.

2 Downlink SCMA system structure

The system structure belonging to the downlink SCMA is illustrated in Fig. 1. At the transmitting part of the relevant scheme given in Fig. 1, each individual user is allocated a particular codebook consisting of M complex codewords each of which has K dimensions. In these $K\times M$-sized codebooks predefined for J different users, the value of M corresponds to the modulation order of the SCMA system. Apart from this, the aforementioned K-dimensional complex codewords forming the columns of $K\times M$-sized codebooks are specified as sparse vectors. Each of these sparse vectors has N non-zero components such that $K > N$. It should be noted that the non-zero elements occupy particular codeword dimensions that do not change within a certain codebook.

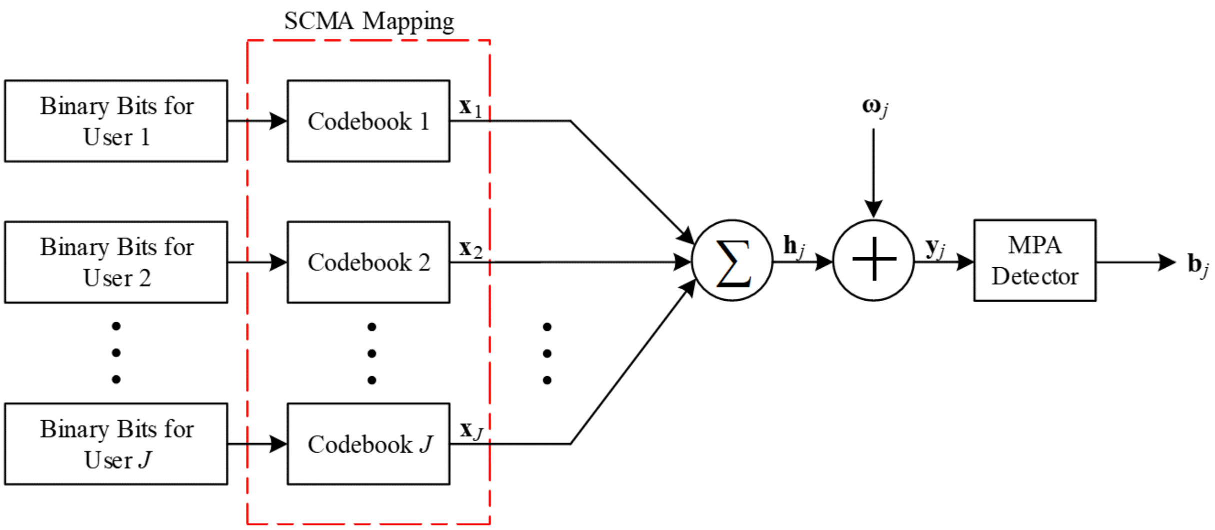

Fig. 1. Block diagram of the downlink SCMA system

SCMA-based data transmission starts with the mapping process in which the m bit information belonging to the user j for (j = 1, 2, …, J) is mapped to the relevant complex codeword existing in the j-th codebook. Upon completing the mapping operation for each user, a superimposed codeword without sparsity is obtained by combining J complex codewords selected from J different codebooks with respect to the information bits of J individual users [28]. The way of mapping information bits to the complex codewords and combining these selected sparse codewords into a single non-sparse codeword is demonstrated in Fig. 2 for $K = 4$, $J = 6$ and $m = 2$. In the codebook illustration given in Fig. 2, the rectangular boxes with different colors indicate non-zero elements while the remaining white boxes represent zero elements [28].

We can use a factor graph for the SCMA system to represent its sparsity scheme. In the following equation, an example of a factor graph representation is given [15]:

$$\boldsymbol{F} = \begin{bmatrix} 0 & 1 & 1 & 0 & 1 & 0 \\ 1 & 0 & 1 & 0 & 0 & 1 \\ 0 & 1 & 0 & 1 & 0 & 1 \\ 1 & 0 & 0 & 1 & 1 & 0 \end{bmatrix} \quad (1)$$

where the rows denote the orthogonal resources and columns indicate the users. Note that each complex codeword existing in a codebook includes K orthogonal resource elements (REs). In this factor graph example given in Eqn. (1), each user occupies two orthogonal resources and these occupied positions are depicted by ones.

For the downlink SCMA system shown in Fig. 1, the expression of the received signal belonging to the j-th user is as follows:

$$\boldsymbol{y}_j = \mathrm{diag}(\mathbf{h}_j) \sum_{j=1}^{J} \boldsymbol{x}_j + \boldsymbol{\omega}_j \tag{2}$$

where

$$\boldsymbol{h}_j = (h_{j1}, h_{j2}, \ldots, h_{jK})^T \text{ and } \boldsymbol{x}_j = (x_{j1}, x_{j2}, \ldots, x_{jK})^T$$

are the channel coefficients and sparse codeword of user j, respectively, while $\boldsymbol{\omega}_j$ represents $K\times 1$-sized complex Gaussian noise vector belonging to the j-th user. Sparsity of the factor graph, an example of which is given in Eqn. (1), makes the SCMA receiver perform a multiuser detection process by utilizing the MPA.

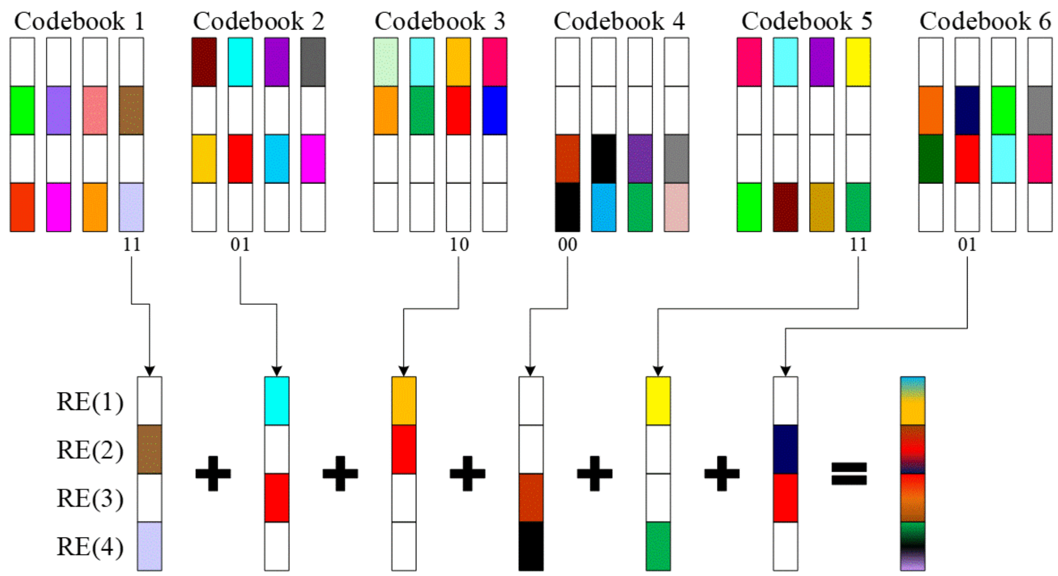

Fig. 2. The operation of mapping and combining performed at the SCMA transmitter

3 Salp swarm algorithm

The salps that belong to the Salpidae family are very interesting marine organisms showing quite similar features to jellyfishes by having a transparent body tissue in cylindrical form and pumping the water through their body to not only move in the ocean but also feed by using their inherent biological filters [29]. While foraging in deep oceans, these amazing creatures show a very different swarming behavior by arranging one after another in a spiral shape, which is called salp chain in literature. Inspired by the aforementioned swarming behaviors of the salps, Mirjalili et al. have produced a novel swarm intelligence-based optimizer called salp swarm algorithm (SSA) by mathematically modelling the strategic foraging movements of these organisms in the form of salp chains [13].

In the SSA, the population is considered to have one leader salp existing at the leading position of the salp chain. The remaining part of the salp population is considered as the followers. In the guidance of the leader salp, the follower salps track each other in the form of salp chain during the foraging process. As in the other population-based algorithms, solution vectors corresponding to the salp positions are defined in a search space with n dimensions. Therefore, each salp position is expressed as n-dimensional solution vector. Apart from this, it is presumed that there exists a target food denoted by f to be reached by the salp chain within the search space. Below is the mathematical model used in the SSA for updating the leader position:

$$s_n^1 = \begin{cases} f_n + r_1 \cdot [(ub_n - lb_n) \cdot r_2 + lb_n], r_3 \geq 0 \\ f_n - r_1 \cdot [(ub_n - lb_n) \cdot r_2 + lb_n], r_3 < 0 \end{cases} \tag{3}$$

where s_n^1, f_n, ub_n and lb_n indicate the leader (first) salp position, target food position, upper bound and lower bound in the n-th dimension, respectively. r_3 and r_2 are the random values generated in the ranges [−1, 1] and [0, 1], respectively while r_1 is a coefficient that is updated with respect to the iteration number throughout the optimization process in the following way:

$$r_1 = 2 \cdot \mathrm{e}^{-\left(\frac{4k}{I_{\max}}\right)^2} \tag{4}$$

where k and $I_{\max}$ represent current and maximum iteration numbers, respectively. It should be noted that r_1 is the main control parameter ensuring the SSA to balance exploitation and exploration during the search for the optimal solution. In order to update the follower salp positions, the law of motion proposed by Newton is utilized as follows:

$$s_n^i = \frac{1}{2} \cdot \alpha \cdot t^2 + \beta_0 \cdot t, i = 2,3,\ldots,P \quad (5)$$

where the n-th dimension of the i-th follower salp position is signified by s_n^i, β_0 corresponds to the initial speed, $\alpha = \beta_{final}/\beta_0$, t denotes time, $\beta = (s - s_0)/t$ and P is the size of salp population. In the optimization process, the time is equivalent to iteration. Since the difference between the iterations equals 1, Eqn. (5) can be modified by considering $\beta_0 = 0$ in the following manner:

$$s_n^i = \frac{1}{2} \cdot \left(s_n^i + s_n^{i-1}\right), i = 2,3,\ldots,P \quad (6)$$

The working principle of SSA can be easily comprehended from its pseudo-code given in Fig. 3.

```
Randomly generate initial salp positions s^i (i = 1,2,...,P)
complying with lb and ub
while (termination criterion is not met)
    Perform fitness calculation for each salp position
    Assign the best individual as the target food position f
    Update the parameter r1 via Eqn. (4)
    for each salp (s^i)
        if (i == 1)
         Update the leader salp position via Eqn. (3)
        else
         Update the follower salp positions via Eqn. (6)
        end
    end
    Fix the new salp positions with respect to lb and ub values
end
Return f
```

Fig. 3. The pseudo-code of SSA

The key advantages of SSA algorithm can be summarized as follows [13]:

- The best salp position achieved so far is saved as the target food position. By doing so, the current best solution vector corresponding to the target food position is always protected and never lost throughout the optimization process even if the salp population deviates from the global optimum as a whole.
- The space around the current best solution is always explored and exploited via the leader salp, the position of which is updated with respect to the best solution achieved so far.
- The position update mechanism defined for the follower salps in Eqn. (6) leads to a gradual movement towards the leader salp, which prevents the SSA from getting easily stuck in local optimum.
- The adaptive reduction of parameter r_1 throughout the iterations makes the SSA algorithm to effectively scan the search space by first exploring and then exploiting it.
- SSA algorithm has easy to implement and simple structure by possessing just one main control parameter, which is r_1.

4 Design of codebook using salp swarm algorithm

As previously mentioned in this paper, we appoint the average BER of the SCMA scheme as the fitness function of the SSA algorithm. When optimizing the codebook set by employing the proposed metaheuristic approach, we will utilize the following notations [15]:

$$p_j^2 + q_j^2 = E \quad (7)$$

$$\frac{p_j^2}{q_j^2} = \lambda_j, j = 1,2,\ldots,J \quad (8)$$

where p_j and q_j represent the symbol magnitudes belonging to the codewords, E corresponds to the energy of a codeword and λ_j specifies the variation of codeword power. In this study, the value of codeword energy denoted by E is kept at 1 for the purpose of making every single codeword of the designed codebooks to have unit norm. It is worth mentioning that the convergence efficiency of the MPA detector used at the SCMA receiver for symbol detection enhances with power variations in orthogonal resources and these power variations can be achieved by ensuring the parameter λ_j to have varying values among the codebooks of different users. With the usage of Eqns. (7) and (8), it is possible to express p_j and q_j parameters in terms of λ_j and E as shown in the equations below:

$$\frac{1}{q_j^2} \cdot \left(p_j^2 + q_j^2\right) = \frac{1}{q_j^2} \cdot E \Rightarrow \lambda_j + 1 = \frac{E}{q_j^2}$$
$$\Rightarrow q_j^2 = \frac{E}{\lambda_j + 1} \Rightarrow \lambda_j \cdot q_j^2 = \frac{E \cdot \lambda_j}{\lambda_j + 1} \Rightarrow p_j^2 = \frac{E \cdot \lambda_j}{\lambda_j + 1}$$
$$\Rightarrow p_j = \sqrt{\frac{E \cdot \lambda_j}{(\lambda_j + 1)}} \quad (9)$$

$$\frac{1}{q_j^2} \cdot \left(p_j^2 + q_j^2\right) = \frac{1}{q_j^2} \cdot E \Rightarrow \lambda_j + 1 = \frac{E}{q_j^2}$$
$$\Rightarrow q_j^2 = \frac{E}{\lambda_j + 1} \Rightarrow q_j = \sqrt{\frac{E}{(\lambda_j + 1)}} \quad (10)$$

The codebooks belonging to different users can be modelled in a generalized form for $j > 1$ as follows:

$$\boldsymbol{C}_j = \begin{bmatrix} 0 & 0 & 0 & 0 \\ p_j e^{i\cdot\theta_v} & -q_j e^{i\cdot\theta_v} & q_j e^{i\cdot\theta_v} & -p_j e^{i\cdot\theta_v} \\ -q_j e^{i\cdot\theta_{v+1}} & -p_j e^{i\cdot\theta_{v+1}} & p_j e^{i\cdot\theta_{v+1}} & q_j e^{i\cdot\theta_{v+1}} \\ 0 & 0 & 0 & 0 \end{bmatrix} \quad (11)$$

where $j = 1, 2, \ldots, J$ and $v = 2l$ for $l = 1, 2, \ldots, J-1$. Apart from the initial non-zero row of $\mathbf{C}_1$ matrix indicating the codebook of first user, the non-zero rows of each codebook are multiplied by $e^{i\cdot\theta_v}$ complex exponent. In the case that the factor graph yielded in Eqn. (1) is utilized, we can model the codebook set for $J = 6$ users in the following way:

$$\boldsymbol{C}_1 = \begin{bmatrix} 0 & 0 & 0 & 0 \\ p_1 & -q_1 & q_1 & -p_1 \\ 0 & 0 & 0 & 0 \\ -q_1 e^{i\cdot\theta_1} & -p_1 e^{i\cdot\theta_1} & p_1 e^{i\cdot\theta_1} & q_1 e^{i\cdot\theta_1} \end{bmatrix} \quad (12)$$

$$\boldsymbol{C}_2 = \begin{bmatrix} p_2 e^{i\cdot\theta_2} & -q_2 e^{i\cdot\theta_2} & q_2 e^{i\cdot\theta_2} & -p_2 e^{i\cdot\theta_2} \\ 0 & 0 & 0 & 0 \\ -q_2 e^{i\cdot\theta_3} & -p_2 e^{i\cdot\theta_3} & p_2 e^{i\cdot\theta_3} & q_2 e^{i\cdot\theta_3} \\ 0 & 0 & 0 & 0 \end{bmatrix} \quad (13)$$

$$\boldsymbol{C}_3 = \begin{bmatrix} p_3 e^{i\cdot\theta_4} & -q_3 e^{i\cdot\theta_4} & q_3 e^{i\cdot\theta_4} & -p_3 e^{i\cdot\theta_4} \\ -q_3 e^{i\cdot\theta_5} & -p_3 e^{i\cdot\theta_5} & p_3 e^{i\cdot\theta_5} & q_3 e^{i\cdot\theta_5} \\ 0 & 0 & 0 & 0 \\ 0 & 0 & 0 & 0 \end{bmatrix} \quad (14)$$

$$\boldsymbol{C}_4 = \begin{bmatrix} 0 & 0 & 0 & 0 \\ 0 & 0 & 0 & 0 \\ p_4 e^{i\cdot\theta_6} & -q_4 e^{i\cdot\theta_6} & q_4 e^{i\cdot\theta_6} & -p_4 e^{i\cdot\theta_6} \\ -q_4 e^{i\cdot\theta_7} & -p_4 e^{i\cdot\theta_7} & p_4 e^{i\cdot\theta_7} & q_4 e^{i\cdot\theta_7} \end{bmatrix} \quad (15)$$

$$\boldsymbol{C}_5 = \begin{bmatrix} p_5 e^{i\cdot\theta_8} & -q_5 e^{i\cdot\theta_8} & q_5 e^{i\cdot\theta_8} & -p_5 e^{i\cdot\theta_8} \\ 0 & 0 & 0 & 0 \\ 0 & 0 & 0 & 0 \\ -q_5 e^{i\cdot\theta_9} & -p_5 e^{i\cdot\theta_9} & p_5 e^{i\cdot\theta_9} & q_5 e^{i\cdot\theta_9} \end{bmatrix} \quad (16)$$

$$\boldsymbol{C}_6 = \begin{bmatrix} 0 & 0 & 0 & 0 \\ p_6 e^{i\cdot\theta_{10}} & -q_6 e^{i\cdot\theta_{10}} & q_6 e^{i\cdot\theta_{10}} & -p_6 e^{i\cdot\theta_{10}} \\ -q_6 e^{i\cdot\theta_{11}} & -p_6 e^{i\cdot\theta_{11}} & p_6 e^{i\cdot\theta_{11}} & q_6 e^{i\cdot\theta_{11}} \\ 0 & 0 & 0 & 0 \end{bmatrix} \quad (17)$$

In the SSA-based codebook design procedure, the optimum set of codebooks minimizing the average BER of the SCMA scheme is obtained by optimizing the following vector parameters via the SSA algorithm:

$$\boldsymbol{\lambda} = (\lambda_1, \lambda_2, \ldots, \lambda_J) \quad (18)$$

$$\boldsymbol{\theta} = (\theta_1, \theta_2, \ldots, \theta_{JN-1}) \quad (19)$$

where N denotes the number of non-zero components existing in each column of the codebook matrices. As it is evident from the lengths of $\boldsymbol{\lambda}$ and $\boldsymbol{\theta}$ vectors, a total of $(JN + J - 1)$ parameters are required to be optimized by the SSA. For instance, we will need to optimize 6×2+6–1=17 parameters for N=2 non-zero components per matrix column and $J = 6$ users. For these J and N values, the vectors of $\boldsymbol{\lambda}$ and $\boldsymbol{\theta}$ will transform into the following form:

$$\boldsymbol{\lambda} = (\lambda_1, \lambda_2, \ldots, \lambda_6) \quad (20)$$

$$\boldsymbol{\theta} = (\theta_1, \theta_2, \ldots, \theta_{11}) \quad (21)$$

The above vector parameters will be optimized in this study with the utilization of SSA algorithm. Below is the definition of fitness function that needs to be minimized throughout the optimization process:

$$fitness = BER\left(\boldsymbol{F}, \boldsymbol{\lambda}, \boldsymbol{\theta}, \frac{E_b}{N_0}\right) \quad (22)$$

By using a predefined factor graph $\mathbf{F}$ for the λ and θ parameters that are subjected to the optimization process, the $BER(\cdot)$ function calculates the average bit error rate in the downlink SCMA scheme at a pre-determined value of E_b / N_0 corresponding to energy per bit-to-noise ratio. In the simulations, we use the factor graph $\mathbf{F}$ provided in Eqn. (1). Besides, after it was realized as a result of repetitive simulations that the best optimization results are obtained at 12 dB E_b / N_0 value for the Rayleigh fading channel, the value of parameter E_b / N_0 is kept at 12 dB while the codebook set is being optimized. Apart from this, the optimization boundaries determined for the λ and θ parameters are as follows [15]:

$$\left.\begin{matrix} 0 \le \theta_v < 2\pi, & v = 1,2,\ldots,JN-1 \\ 0.01 \le \lambda_j \le 40, & j = 1,2,\ldots,J \end{matrix}\right\} \quad (23)$$

In the course of optimizing the codebook set, when the fitness value is to be calculated in a certain iteration, the set of codebooks is obtained with respect to the current λ and θ values by using the Eqns. (12-17), which are defined based on these parameters. Thereafter, for the relevant iteration, the average BER of the SCMA scheme (fitness value) is calculated by employing the obtained set of codebooks. The iterations are kept going until we reach a codebook set ensuring the minimum BER (fitness) value. In the next subsection, the operation steps belonging to the SSA-based codebook optimization are presented in detail.

4.1 Step by step description of the codebook optimization based on SSA algorithm

First of all, in order to make λ and θ parameters ready for being optimized via the SSA algorithm, these parameter sequences specified in Eqns. (18) and (19) are merged into a single vector, which is defined as the ith salp position in the following way:

$$s_n^i = [\lambda_1^i, \lambda_2^i, \ldots, \lambda_J^i, \theta_1^i, \theta_2^i, \ldots, \theta_{JN-1}^i]$$
$$i = 1,2,\ldots,P; n = 1,2,\ldots,JN + J - 1 \quad (24)$$

where i is the salp index and P is the size of salp population.

Step 1: Random positions are assigned to the initial salp population by considering the boundaries defined for λ and θ variables in Eqn. (23).

Step 2: The fitness values of the salp positions are obtained by utilizing the fitness function specified in Eqn. (22).

Step 3: The best individual position possessing the greatest fitness quality in the current salp population is assigned as the position of target food source as follows:

$$f_n = s_n^* = [\lambda_1^*, \lambda_2^*, \ldots, \lambda_J^*, \theta_1^*, \theta_2^*, \ldots, \theta_{JN-1}^*] \quad (25)$$

where the target food position f_n is made equal to the best salp position symbolized by s_n^*.

Step 4: The parameter r_1 is updated using Eqn. (4).

Step 5: Position update is carried out for each salp:

5.1. if $i = 1$

- The position of leader salp s_n^1 is updated using Eqn. (3).

5.2. else if $i > 1$

- The positions of follower salps are updated using Eqn. (6).

Step 6: The new positions produced for the population members are adjusted with respect to the lower and upper bounds defined for each vector parameters in Eqn. (23).

Step 7: If the maximum number of iterations denoted by I_{max} has not been reached yet, the optimization process keeps going from Step 2. Otherwise, the latest target food position f_n is appointed as the optimum solution vector acquired at the end of I_{max} iterations. In order to eventually obtain the SSA-based designed codebook set, the optimized values of λ and θ parameters comprising the related solution vector is utilized. To this end, after λ parameters are employed in Eqns. (9) and (10) to obtain p and q symbol magnitudes, these symbol magnitudes obtained with respect to the λ parameters are employed together with the θ parameters in Eqns. (12-17) to achieve the eventual set of codebooks optimized by the SSA algorithm.

5 Simulation results

In this section, an experimental analysis is carried out to test our SSA-based designed codebook set in point of BER performance in the downlink SCMA scheme. In order to see how satisfactory the BER results of the proposed codebook set are, we compare its BER performance to those of diversified successful set of codebooks available in the literature such as AESCMA [25], LowError [18], Hu [26], Huawei and ConsRot [27]. In the simulations, the system parameters are specified as indicated in Tab. 1.

Table 1. System parameters

Parameter	Symbol	Value
Number of users	J	6
Number of codewords per codebook	M	4
Number of orthogonal resources	K	4
Number of non-zero components per codeword	N	2
Type of wireless channel	-	Rayleigh fading
Type of detecting algorithm	-	Log-MPA
Number of iterations for Log-MPA	-	5
Size of population for SSA	P	10
Maximum iteration number for SSA	I_{max}	25

The eventual values of λ and θ vector parameters acquired at the end of SSA-based optimization process are provided in the following equations:

$$\boldsymbol{\lambda} = \begin{pmatrix} 28.1826,\ 19.2281,\ 7.5434,\ 23.7980,\ldots \\ 13.6350,\ 16.8980 \end{pmatrix} \quad (26)$$

$$\boldsymbol{\theta} = \begin{pmatrix} 5.1982,\ 4.6688,\ 3.8480,\ 3.9161, 1.2478,\ldots \\ 2.1915,\ 6.1163,\ 5.6580,\ 3.8170, 4.6869,\ldots \\ 5.8309 \end{pmatrix} \quad (27)$$

After utilizing the above optimized λ and θ parameters, the corresponding SSA-based codebook set is obtained as follows:

$$\boldsymbol{C}_1 = \begin{bmatrix} 0 & 0 & 0 & 0 \\ 0.9827 & -0.1851 & 0.1851 & -0.9827 \\ 0 & 0 & 0 & 0 \\ -0.0864+0.1637i & -0.4589+0.8690i & 0.4589-0.8690i & 0.0864-0.1637i \end{bmatrix} \quad (28)$$

$$\boldsymbol{C}_2 = \begin{bmatrix} -0.0424-0.9740i & 0.0097+0.2221i & -0.0097-0.2221i & 0.0424+0.9740i \\ 0 & 0 & 0 & 0 \\ 0.1691+0.1443i & 0.7417+0.6329i & -0.7417-0.6329i & -0.1691-0.1443i \\ 0 & 0 & 0 & 0 \end{bmatrix} \quad (29)$$

$$\boldsymbol{C}_3 = \begin{bmatrix} -0.6716-0.6571i & 0.2445+0.2393i & -0.2445-0.2393i & 0.6716+0.6571i \\ -0.1086-0.3244i & -0.2983-0.8911i & 0.2983+0.8911i & 0.1086+0.3244i \\ 0 & 0 & 0 & 0 \\ 0 & 0 & 0 & 0 \end{bmatrix} \quad (30)$$

$$\boldsymbol{C}_4 = \begin{bmatrix} 0 & 0 & 0 & 0 \\ 0 & 0 & 0 & 0 \\ -0.5697+0.7969i & 0.1168-0.1634i & -0.1168+0.1634i & 0.5697-0.7969i \\ -0.1980+0.0334i & -0.9660+0.1627i & 0.9660-0.1627i & 0.1980-0.0334i \end{bmatrix} \quad (31)$$

$$\boldsymbol{C}_5 = \begin{bmatrix} 0.7826-0.5649i & -0.2120+0.1530i & 0.2120-0.1530i & -0.7826+0.5649i \\ 0 & 0 & 0 & 0 \\ 0 & 0 & 0 & 0 \\ 0.2040+0.1634i & 0.7533+0.6035i & -0.7533-0.6035i & -0.2040-0.1634i \end{bmatrix} \quad (32)$$

$$\boldsymbol{C}_6 = \begin{bmatrix} 0 & 0 & 0 & 0 \\ -0.0248-0.9713i & 0.0060+0.2363i & -0.0060-0.2363i & 0.0248+0.9713i \\ -0.2126+0.1033i & -0.8740+0.4246i & 0.8740-0.4246i & 0.2126-0.1033i \\ 0 & 0 & 0 & 0 \end{bmatrix} \quad (33)$$

In Fig. 4, the codebook sets considered in this paper are compared with each other in terms of their BER achievements in the downlink SCMA system. The curves that exist in the relevant figure are the average BER curves belonging to the considered codebook sets. While obtaining the related curves, six different BER values belonging to six different users of the SCMA scheme are obtained and then averaged for each value of E_b / N_0 in the range 0 dB to 22 dB. As it is evident from Fig. 4, our proposed SSA-based designed codebook set leaves the other ones behind by a clear distance. It manages to make 1.29 dB difference even to its nearest competitor named ConsRot at 10^{-3} BER level. Apart from this, even though the AESCMA, LowError and Hu show better BER performance compared to the Huawei and ConsRot at low E_b / N_0 values approximately in the range 0 dB to 12 dB, these three codebook sets fall far behind the other ones at higher E_b / N_0 values beyond 14 dB. Starting from 14 dB E_b / N_0 value, the BER curves of the considered codebook sets are separated into two distinct groups. While Huawei, ConsRot and SSA form the group of codebooks that perform better, the worse performer codebook group consists of AESCMA, LowError and Hu. As can be seen in Fig. 4, the distance between these two groups widens as the value of E_b / N_0 increases.

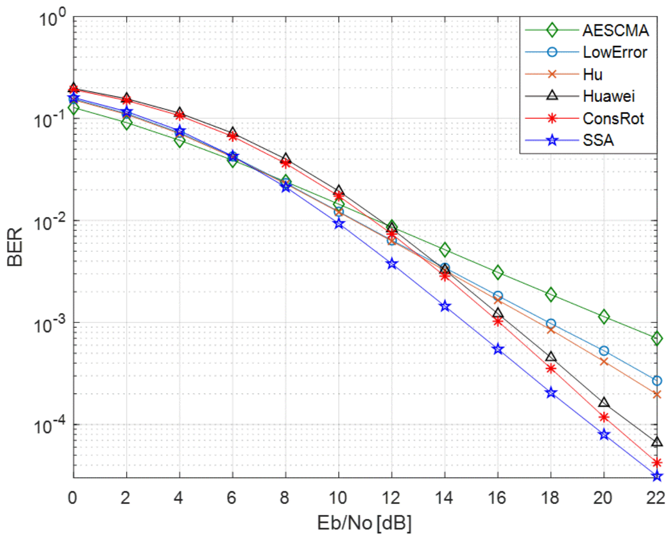

Fig. 4. The performance of codebook sets in terms of average BER achievements in the downlink SCMA system

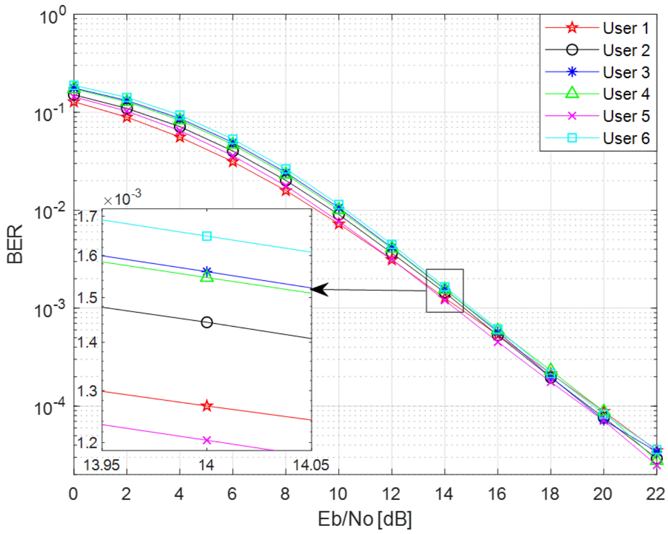

Fig. 5. User-based performance analysis of the SSA-based codebook set

In Fig. 5, the BER performance is analyzed for each user individually in the case that our proposed codebook set designed by using the SSA algorithm is employed in the downlink SCMA system. In general, the effectiveness of a codebook set is evaluated with respect to its average BER performance. This is the primary metric to be considered when determining the capacity of a designed codebook set. On the other hand, the BER achievements of individual users should also be taken into account to see whether a codebook set is feasible for practical scenarios. In real life applications, every user is expected to get a communication service with similar quality standard. For this to happen, the BER curves of the individual users are required to be in close proximity to each other. The proposed SSA-based codebook set meets this criterion. As can be seen from Fig. 5, the BER curves belonging to multiple users are quite close to each other. They are even almost overlapping at higher E_b / N_0 values. From this perspective, not only being superior over the other considered codebook sets with regard to average BER performance, but also providing quite similar BER results for the individual users makes the SSA an advantageous codebook set that deserves to be taken into consideration for being exploited in the downlink SCMA scheme.

Figure 6 presents the BER achievements belonging to worst and best users of the codebook sets considered in this paper. As mentioned earlier, even though the main performance metric to look at when conducting a performance evaluation for a codebook set is the average BER achievement of the multiple users, it is undesirable for individual users to show great deal of variability in their BER performances. For this reason, the BER curves of worst and best users are expected to be close to each other as much as possible. When we look at Fig. 6, it will be seen that AESCMA, LowError and Hu have the larger distances between their worst and best users compared to the other three set of codebooks named Huawei, ConsRot and SSA. Meanwhile, it is worth reminding that the aforementioned three codebook sets having great deal of differences between their worst and best users also stand out from the others by showing worse average BER performance as can be observed from Fig. 4. If we examine Fig. 6 more closely, we will see that our proposed SSA has been the second codebook set providing the lowest difference between the curves of worst and best users, while Huawei ranks the first in this respect. However, in spite of having multiple users with very close BER performances, Huawei falls far behind our proposed SSA-based codebook design strategy with regard to average BER performance, which is the primary criterion that determines the capability of a codebook set.

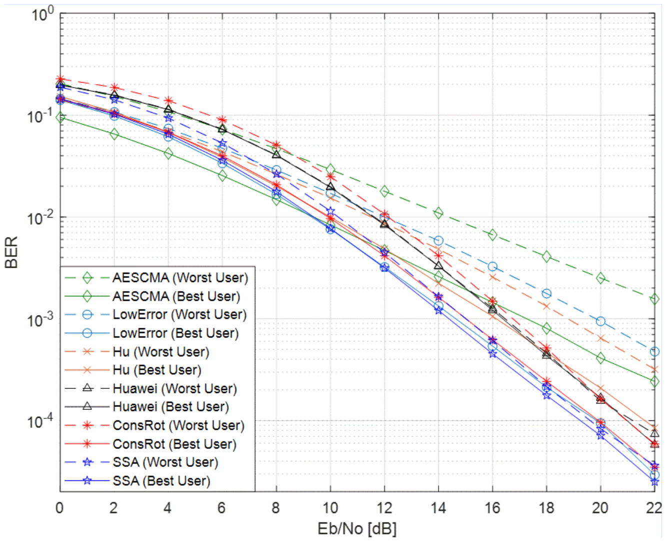

Fig. 6. Worst and best user performances for each set of code-ooks

Figure 7 demonstrates the convergence performance shown by the SSA algorithm while optimizing the set of codebooks in the downlink SCMA system. In this convergence graph, the number of iterations increasing from 0 to 25 is represented by the horizontal axis while the vertical axis displays 10^3 times the average BER values achieved by the SSA algorithm throughout the progress of iterations. As can be noticed from Fig. 7, the convergence curve starts from between 4.2×10^{-3} and 4.3×10^{-3} BER values and suddenly drops below 3.9×10^{-3} at 9th iteration. From that point to the 19th iteration, SSA algorithm reaches below 3.7×10^{-3} by maintaining to converge, gradually. After one last sharp decline from 3.68×10^{-3} to 3.50×10^{-3} BER value at 20th iteration, the convergence of SSA algorithm comes to an end.

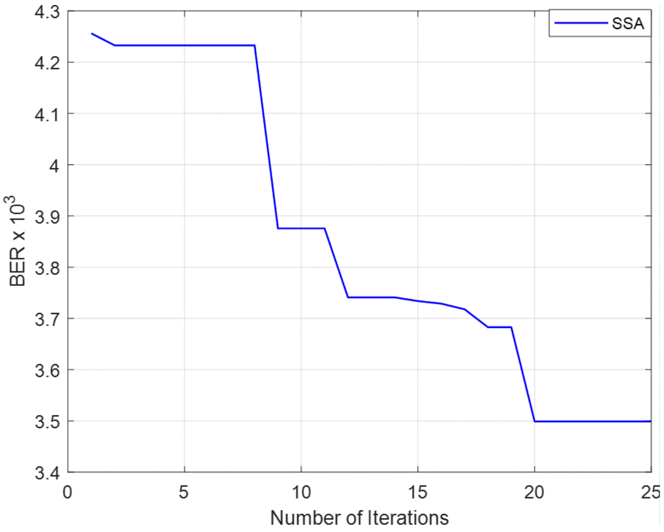

Fig. 7. Convergence performance of SSA while optimizing the codebook set

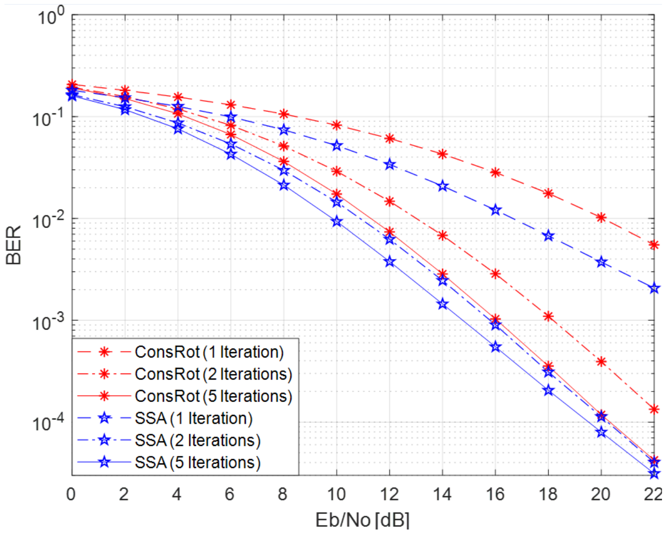

Fig. 8. BER achievements of SSA and ConsRot codebook sets for different iteration numbers of log-MPA detector

In Fig. 8, the BER achievements of the proposed SSA-based codebook set and its closest competitor named ConsRot are analyzed for different number of decoding iterations of the log-MPA detector employed at the SCMA receiver. As can be evidently observed from Fig. 8, our designed set of codebooks keeps its superiority over the ConsRot for each of the considered iteration numbers determined as 1, 2 and 5 for this simulation. Apart from this, a certain number of iterations are needed in the log-MPA detector to perform an accurate symbol detection process. We can see this from the BER results obtained for both SSA and ConsRot codebook sets by varying the number of iterations in log-MPA detector. As can be clearly seen from the BER curves, the growing number of iterations leads to an enhanced BER performance in the downlink SCMA scheme for both of the considered codebook sets. On the other hand, it can be noticed from the distances between the BER curves obtained for different numbers of iterations that the amount of improvement in the BER performance of the downlink SCMA scheme gradually decreases with the increase of iteration number regardless of the codebook set employed at the transmitter side. For instance, if we look at the E_b / N_0 gains achieved for each increment in the number of iterations at 10^{-2} BER level, we will see that 7.05 dB and 5.77 dB gains are achieved for ConsRot and SSA, respectively with the increase of iteration number from 1 to 2 while the related gains reduce to 1.72 dB and 1.05 dB in case of increasing the number of iterations from 2 to 5. We can infer from these results that it is unnecessary to determine too high iteration numbers for the log-MPA detector since its performance reaches saturation after a certain number of iterations.

6 Conclusion

This research presents an efficient strategy based on SSA algorithm to design an appropriate codebook set for the downlink SCMA scheme. In this proposed codebook design strategy, the codebooks of the SCMA scheme can be directly optimized via the SSA algorithm by eliminating the requirement for a mother constellation while designing a codebook set. Furthermore, contrary to many codebook design studies in which only the transmitter part of SCMA is considered by focusing on just the key performance indicators like MPD and MED of the codewords to maximize, we use average BER of the system as the objective function of SSA to minimize. By doing so, it becomes possible to take the whole system with all its components including the log-MPA detector into account when performing the SSA-based optimization on the set of codebooks since the BER achievement of a codebook set is not only determined by the distance properties of the codewords belonging to different codebooks but also affected by the performance of log-MPA-based symbol detecting process carried out at the SCMA receiver. In the simulations, SSA-based codebook set is subjected to a performance measurement together with the other considered ones. To this end, the BER achievements of the existing codebook sets in the case they are employed in the downlink SCMA system are compared to each other. It is explicitly demonstrated by the comparative performance analysis that the proposed set of codebooks designed by utilizing the SSA algorithm enables the downlink SCMA scheme to achieve lower BER levels in comparison to the other considered alternative codebook sets. These promising results achieved by our designed codebook set clearly verifies the efficiency of SSA-based codebook design strategy proposed in this paper.

As possible future works, while BER is minimized, MED can be maximized simultaneously during the codebook optimization by utilizing the multi-objective algorithms. Aside from that, it is possible to utilize the proposed SSA-based codebook design procedure for the other prominent types of fading channel such as Rician, Nakagami, etc., and achieve the optimal codebook set for each one. Furthermore, a unique codebook set that yields satisfying results in the SCMA system for more than one type of channel can be designed by performing a joint optimization procedure.

Acknowledgement

This work was supported by the Scientific Research Projects Coordinating Unit of Nevşehir Hacı Bektaş Veli University [Grant Number: GAP25F04].

References

[1] W. Jiang, Q. Zhou, J. He, M. A. Habibi, S. Melnyk, and M. El-Absi, "Terahertz communications and sensing for 6G and beyond: A comprehensive review," IEEE Communications Surveys & Tutorials, vol. 26, no. 4, pp. 2326-2381, 2024.

[2] R. Ahmed, and M. A. Matin, "Towards 6G wireless networks-challenges and potential technologies," Journal of Electrical Engineering, vol. 71, no. 4, pp. 290-297, 2020.

[3] S. K. Saraswat, V. K. Deolia, and A. Shukla, "Allocation of power in NOMA based 6G-enabled internet of things using multi-objective based genetic algorithm," Journal of Electrical Engineering, vol. 74, no. 2, pp. 95-101, 2023.

[4] N. Abu-Ali, A. E. M. Taha, M. Salah, and H. Hassanein, "Uplink scheduling in LTE and LTE-advanced: Tutorial, survey and evaluation framework," IEEE Communications Surveys & Tutorials, vol. 16, no. 3, pp. 1239-1265, 2013.

[5] L. Dai, B. Wang, Y. Yuan, S. Han, I. Chih-lin, and Z. Wang, "Non-orthogonal multiple access for 5G: solutions, challenges, opportunities, and future research trends," IEEE Communications Magazine, vol. 53, no. 9, pp. 74-81, 2015.

[6] Z. Wei, J. Yuan, D. W. K. Ng, M. Elkashlan, and Z. Ding, "A survey of downlink non-orthogonal multiple access for 5G wireless communication networks," ZTE Communications, vol. 14, no. 4, pp. 17-25, 2016.

[7] Q. Wang, R. Zhang, L.-L. Yang, and L. Hanzo, "Non-orthogonal multiple access: A unified perspective," IEEE Wireless Communications, vol. 25, no. 2, pp. 10-16, 2018.

[8] M. S. Ali, H. Tabassum, and E. Hossain, "Dynamic user clustering and power allocation for uplink and downlink non-orthogonal multiple access (NOMA) systems," IEEE access, vol. 4, pp. 6325-6343, 2016.

[9] S. R. Islam, N. Avazov, O. A. Dobre, and K. S. Kwak, "Power-domain non-orthogonal multiple access (NOMA) in 5G systems: Potentials and challenges," IEEE Communications Surveys & Tutorials, vol. 19, no. 2, pp. 721-742, 2016.

[10] Z. Yang, Z. Ding, P. Fan, and N. Al-Dhahir, "A general power allocation scheme to guarantee quality of service in downlink and uplink NOMA systems," IEEE Transactions on Wireless Communications, vol. 15, no. 11, pp. 7244-7257, 2016.

[11] Y. Wu, C. Wang, Y. Chen, and A. Bayesteh, "Sparse code multiple access for 5G radio transmission," IEEE 86th Vehicular Technology Conference (VTC-Fall), Toronto, ON, Canada, pp. 1-6, 2017.

[12] F. R. Kschischang, B. J. Frey, and H. A. Loeliger, "Factor graphs and the sum-product algorithm," IEEE Transactions on Information Theory, vol. 47, no. 2, pp. 498-519, 2001.

[13] S. Mirjalili, A. H. Gandomi, S. Z. Mirjalili, S. Saremi, H. Faris, and S. M. Mirjalili, "Salp swarm algorithm: A bio-inspired optimizer for engineering design problems," Advances in Engineering Software, vol. 114, pp. 163-191, 2017.

[14] L. Yu, P. Fan, D. Cai, and Z. Ma, "Design and analysis of SCMA codebook based on Star-QAM signaling constellations," IEEE Transactions on Vehicular Technology, vol. 67, no. 11, pp. 10543-10553, 2018.

[15] V. P. Klimentyev, and A. B. Sergienko, "SCMA codebooks optimization based on genetic algorithm," 23th European Wireless Conference, Dresden, Germany, pp. 191-196, 2017.

[16] J. Peng, W. Chen, B. Bai, X. Guo, and C. Sun, "Joint optimization of constellation with mapping matrix for SCMA codebook design," IEEE Signal Processing Letters, vol. 24, no. 3, pp. 264-268, 2017.

[17] Y. Zhou, Q. Yu, W. Meng, and C. Li, "SCMA codebook design based on constellation rotation," IEEE International Conference on Communications, Paris, France, pp. 1-6, 2017.

[18] C. Huang, B. Su, T. Lin, and Y. Huang, "Downlink SCMA codebook design with low error rate by maximizing minimum Euclidean distance of superimposed codewords," IEEE Transactions on Vehicular Technology, vol. 71, no. 5, pp. 5231 -5245, 2022.

[19] M. Alam, and Q. Zhang, "Designing optimum mother constellation and codebooks for SCMA," IEEE International Conference on Communications (ICC), Paris, France, pp. 1-6, 2017.

[20] T. Lei, S. Ni, N. Cheng, S. Chen, and X. Song, "SCMA codebook for uplink Rician fading channels," IEEE Communications Letters, vol. 27, no. 2, pp. 527-531, 2023.

[21] X. Li, Z. Gao, Y. Gui, Z. Liu, P. Xiao, and L. Yu, "Design of power-imbalanced SCMA codebook," IEEE Transactions on Vehicular Technology, vol. 71, no. 2, pp. 2140-2145, 2022.

[22] H. Nikopour, and H. Baligh, "Sparse code multiple access," IEEE 24th Annual International Symposium on Personal, Indoor, and Mobile Radio Communications (PIMRC), London, UK, pp. 332-336, 2013.

[23] M. Taherzadeh, H. Nikopour, A. Bayesteh, and H. Baligh, "SCMA codebook design," IEEE 80th vehicular technology conference (VTC2014-Fall), Vancouver, BC, Canada, pp. 1-5, 2014.

[24] Q. Luo, Z. Liu, G. Chen, Y. Ma, and P. Xiao, "A novel multitask learning empowered codebook design for downlink SCMA networks," IEEE Wireless Communications Letters, vol. 11, no. 6, pp. 1268-1272, 2022.

[25] J. Lin, S. Feng, Y. Zhang, Z. Yang, and Y. Zhang, "A novel deep neural network based approach for sparse code multiple access," Neurocomputing, vol. 382, pp. 52-63, 2020.

[26] J. Yang, Y. Zeng, and W. Wan, "One-stage SCMA codebook design based on bit error rate criterion," 2024 IEEE 24th International Conference on Communication Technology (ICCT), Chengdu, China, pp. 17-21, 2024.

[27] D. Cai, P. Fan, X. Lei, Y. Liu, and D. Chen, "Multi-dimensional SCMA codebook design based on constellation rotation and interleaving," 2016 IEEE 83rd Vehicular Technology Conference (VTC Spring), Nanjing, China, pp. 1-5, 2016.

[28] Y. Zheng, J. Xin, H. Wang, S. Zhang, and Y. Qiao, "A low-complexity codebook design scheme for SCMA systems over an AWGN channel," IEEE Transactions on Vehicular Technology, vol. 71, no. 8, pp. 8675-8688, 2022.

[29] L. Madin, "Aspects of jet propulsion in salps," Canadian Journal of Zoology, vol. 68, no. 4, pp. 765-777, 1990.

Received 5 May 2026